Research Article

Characterization and Therapeutic Efficiency of a Highly Lytic *Pseudomonas* Phage Against Carbapenem- Resistant *Pseudomonas aeruginosa* Isolated from Egypt

Rabab M. Soliman[1]*, Ahmed B. Barakat[1], Ayman El-Shibiny[2,3], Iman Mohamed Amin Elkholy[4], Ahmed Askora[5] and Marwa M. Gado[1]

[1]Department of Microbiology, Faculty of Science, Ain Shams University, Cairo, Egypt; [2]Center for Microbiology and Phage Therapy, Zewail City of Science and Technology, Giza, 12578, Egypt; [3]Faculty of Environmental Agricultural Sciences, Arish University, Arish, Egypt; [4]Ain Shams Specialized Hospital, Ain Shams University, Abbasya, Cairo, Egypt; [5]Department of Microbiology and Botany, Faculty of Science, Zagazig University, Zagazig 44519, Egypt.

Abstract | *Pseudomonas aeruginosa* is considered as one of the most dangerous microorganisms to public health, causing considerable mortality rates due to its resistance to a range of antibiotics. It causes substantial tissue damage of varying degrees of severity. Its biofilm's buildup leads to repeated infections that are resistant to conventional medications. As a result, alternate antimicrobial therapies are urgently required. Phage therapy has recently emerged as a promising treatment approach due to its potential to eradicate these bacterial infections. In this study, 35 strains of *P. aeruginosa* were obtained from individuals suffering from different infections. These strains were identified using the automated Vitek 2 approach and confirmed by 16S rDNA sequencing. The ability of these strains to form biofilms and their resistance to antibiotics, both phenotypically and genotypically were studied. The *Pseudomonas* phage RM_Ps3 was isolated and characterized. The therapeutic efficacy of this phage was tested using *in vitro* antibacterial and antibiofilm activities. The obtained results revealed that *P. aeruginosa* clinical isolates had carbapenem resistance in their phenotype, confirmed genotypically by the presence of the *blaNDM* carbapenemase-encoding gene in carbapenem-resistant *P. aeruginosa* Ps21. The isolates also had a high multiple antibiotic resistance (MAR) index and a strong potential to form biofilms. The isolated *Pseudomonas* phage had a podoviral morphology related to the Caudoviricetes class, with a short, rigid tail of around 17.8 nm and a capsid of 60 nm, as indicated by Transmission Electron Microscopy (TEM) inspection. The phage's host range was fairly wide; it lysed 86% of clinical isolates studied. Phage RM_Ps3 demonstrated good stability over a range of pH from 3.0 to 11.0, in addition to its capacity to tolerate temperature ranges of up to 70°C. *In vitro*, the *Pseudomonas* phage RM_Ps3 effectively inhibited and eliminated biofilm formation, and considerably limited the bacterial growth. Our findings display that a powerful phage could be a promising treatment for carbapenem- resistant *P. aeruginosa* infections.

Received | November 05, 2025; **Revised** | December 12, 2025; **Accepted** | December 20, 2025; **Published** | December 30, 2025
***Correspondence** | Rabab M. Soliman, Department of Microbiology, Faculty of Science, Ain Shams University, Cairo, Egypt; **Email:** Rababsoliman@sci.asu.edu.eg
Citation | Soliman, R.M., A.B. Barakat, A. El-Shibiny, I.M.A. Elkholy, A. Askora and M.M. Gado. 2025. Characterization and therapeutic efficiency of a highly lytic *Pseudomonas* phage against carbapenem- resistant *Pseudomonas aeruginosa* isolated from Egypt. *Novel Research in Microbiology Journal,* 9(6): 486-504.
DOI | https://dx.doi.org/10.17582/journal.nrmj/2025/9.6.486.504
Keywords | Carbapenem-resistant *P. aeruginosa*, Biofilm formation, *Pseudomonas* phage RM_Ps3, Phage therapy, Antibacterial efficiency, Antibiofilm activity

Introduction

Pseudomonas aeruginosa causes a wide variety of diseases, ranging from soft tissue infections to potentially lethal disorders such as pneumonia and bacteremia. Furthermore, *P. aeruginosa* DNA encodes adaptability and versatility, making it a global opportunistic pathogen and an important driver of nosocomial infections (Abdelghafar *et al*., 2023).

Pseudomonas aeruginosa is resistant to many antibiotics, including aminoglycosides, β-lactams, and fluoroquinolones, in addition to disinfectants. This is due to both acquired and intrinsic resistance mechanisms that are present in this bacterium. Its intrinsic resistance is characterized by reduced membrane permeability, overexpression of efflux pumps that transport antibiotics out of the cell, and creation of enzymes that inhibit the action of antibiotics (Glen and Lamont, 2021). Another crucial virulence factor that has been linked to antibiotic resistance is the biofilms formation, which hinders drug penetration and protects the bacterium from the human immune system response (Chegini *et al*., 2020). Based on a 2019 World Health Organization (WHO) report, resistance to antibiotics leads to 1.27 million deaths globally, with six bacterial species, including *P. aeruginosa*, causing over 80% of these deaths (Ranjbar and Alam, 2023). The Centers for Disease Control and Prevention (CDC) classifies *P. aeruginosa* as a remarkable threat microorganism because of its high death rate (Kadri, 2020). Furthermore, in the Middle East region, Egypt has the highest infection rate for multi-drug resistant (MDR) *P. aeruginosa* (75.6%) (Al-Orphaly *et al*., 2021).

Missing the efficiency of treatment with antibiotics would be fatal, and we are rapidly getting closer to such a crisis so-called "post antibiotic era". Numerous pharmaceutical corporations are no longer actively interested in the discovery of new antibiotics because it would take many years to create them and the newly marketed antibiotics would quickly acquire resistance, resulting in limited profits (Qin *et al*., 2022). As a result, the demand for alternate antibacterial treatments has emerged. Thus, bacteriophages could be a viable option. To treat bacterial infections, bacteriophages were employed as therapeutic agents 20 years ago prior to the first use of antibiotic medication in clinical settings (Ling *et al*., 2022).

Bacteriophages (phages) are viruses that can invade and proliferate in bacterial cells. They are the most prevalent biological members on Earth, with almost 10^{31} members globally (Abedon *et al*., 2017). Most phages comprise a protein head that contains genetic material (DNA) and a hollow tube tail, which permits their DNA to be injected into the host cells (Soliman *et al*., 2023). Phages are effectively treating the MDR challenge *via* their distinctive features, making them potent therapeutic options because they are safe and do not harm the natural flora. Furthermore, as being self-limiting and self-replicating, they continue to emerge and disseminate to deeper infection sites (Taati Moghadam *et al*., 2020; Zalewska-Piątek, 2023).

The Food and Drug Administration (FDA) announced that bacteriophages are generally harmless. They are already present in food and beverages on a daily basis. In the European Union, phages are classified as feed additives and/or processing assistance, while in the United States (US), they are controlled by Generally Recognized As Safe (GRAS) certification, just like other chemical compounds or protein-based preparations (Huang *et al*., 2022; Jordá *et al*., 2023). Numerous different nations, such as New Zealand, Australia, Canada, and Switzerland, have permitted the use of phages based on the US regulatory requirements (Singh *et al*., 2025).

The antibacterial effectiveness of bacteriophages against MDR *P. aeruginosa* was evaluated both *in vitro* and *in vivo* in several studies (Arumugam *et al*., 2022; Alqahtani, 2023; Ata-Vural *et al*., 2025; Mohamed *et al*., 2025). These investigations demonstrated that bacteriophages are highly effective at killing MDR *P. aeruginosa*. One of these studies, reported by Shokri *et al*. (2017), examined phage cocktails against *P. aeruginosa* that are resistant to colistin, and their results indicated that the phage cocktail completely eradicated the colistin-resistant *P. aeruginosa* 1 cells. In another study, Rezk *et al*. (2022) revealed that the phage ZCPA1 had strong lytic activity against MDR *P. aeruginosa* biofilms and planktonic forms. In addition, the rat model showed complete wound healing using phage ZCPA1. Furthermore, Mohamed *et al*. (2025) isolated phage vB_Ps_ZCPS13 as a promising therapeutic agent for pan-drug-resistant *P. aeruginosa*, particularly in biofilm-associated illnesses. In terms of suppressing and eliminating mature biofilms, the phage outperformed expectations, displaying significant lysis alongside 93% of the clinical isolates

examined. The objectives of this study were to isolate, characterize, and investigate the therapeutic efficacy of *Pseudomonas* phage RM_Ps3 against carbapenem-resistant *P. aeruginosa in vitro*.

Materials and Methods

Collection and identification of the bacterial isolates

Over the duration of a year, from July 2023 to July 2024, 47 clinical samples from different sources, including blood (13), wound (15), sputum (9), and urine (10) were collected from suspected *P. aeruginosa* patients that visited Abou Elazayem hospital in Cairo, Egypt. The collected samples were cultured in tryptic soya broth and streaked on tryptic soya agar plates. After incubation for 24 h at 37 °C, separated pure bacterial isolates were exposed to conventional identification steps, including Gram-staining technique, growth on MacConkey and cetrimide agar selective media (Oxoid, England). Biochemical identification of the bacterial isolates was checked using the Vitek-2 automated system (bioMérieux, Marcy l'Étoile, France) (El-Sherif *et al*., 2022). Following identification, the bacterial isolates were stored at -80°C in Tryptic Soy Broth (TSB) mixed with 20% glycerol (Barman *et al*., 2018).

Detection of the Phenotypic and genotypic resistance patterns of the bacterial isolates

The Vitek-2 AST system (BioMérieux, Marcy l'Etoile, France) was employed to evaluate the vulnerability of bacterial isolates to antimicrobial drugs using the Gram-negative bacteria (GNB) susceptibility testing cards and the 2.01 version software (Barman *et al*., 2018). 2 ml of each *P. aeruginosa* isolate suspension were used for the susceptibility assay, and automatically applied to the VITEK-2 AST system. The used antibiotic discs included: ciprofloxacin (5 µg/ml), amikacin (64 µg/ml), tobramycin (16 µg/ml), gentamicin (16 µg/ml), imipenem (16 µg/ml), meropenem (16 µg/ml), ceftazidime (64 µg/ml), cefepime (64 µg/ml), piperacillin (128 µg/ml), piperacillin-tazobactam (128 µg/ml), ticarcillin (128 µg/ml), ticarcillin-clavulanate (128 µg/ml), and colistin (2 µg/ml). Antibiotic susceptibility testing's were evaluated referring to the CLSI standards, which categorized antibiotic susceptibility patterns into three groups: mainly resistant, intermediate, and sensitive (Schuetz *et al*., 2025). In order to determine the multiple antibiotic resistance (MAR) index, divide the number of antimicrobial agents to which a bacterial isolate was not susceptible (either resistant or intermediately susceptible) by the total number of antimicrobial agents used (Krumperman, 1983). The Bio Fire Film Array was employed to explore the genotypic resistance features of the selected *P. aeruginosa* isolate. A sterile disposable sample transfer tool (Copan Flock Technologies, Brescia, Italy) was utilized to transfer 200 mL broth from a positive blood culture to a sample injection vial, and mixed with the sample buffer (Guanidinium chloride and Triton X-100) that was provided. Afterward, the solution (*i.e*., 200 µL of the positive blood broth culture were mixed with the provided sample buffer) was injected into the Film Array pouch, which was inserted into the Film Array device. Within 2 h, the gadget performed nucleic acid extraction, multiplex PCR, and a DNA melting curve analysis to confirm and identify the existence of antibiotic resistance genes (El-Sherif *et al*., 2022).

Detection of biofilm formation using the microtiter plate assay

A microplate reader was used to detect ability of the isolates to form biofilms. After preparing a bacterial suspension in TSB with 1% glucose, 200 µl of the *P. aeruginosa* (10^6 cfu/ml) were injected into on a sterile polystyrene microplate with 96-well flat bottom. All inoculated microplates were incubated at 37 °C for 48 h. After incubation, the planktonic cells were removed, and the wells were washed twice with distilled water. The plates were air dried to enable the biofilms to adhere directly to them. Following staining with 0.1% crystal violet (CV) solution (Solarbio, Beijing, China), 30% acetic acid was used to a de-stain. A microplate reader (BioTek, Synergy, USA) was used to determine the absorbance of each well at 595 nm (Tang *et al*., 2011). Blanks that served as negative controls were inoculated with sterile TSB only. Biofilms were generated by bacterial isolates that recorded optical density (OD) values higher than those of the blank well. OD measurements can be used to differentiate four types of biofilm formation: Non-producers were represented by ODs ≤ ODc, weak producers by ODc ≤ODs ≤2 ×ODc, moderate producers by 2 ×ODc ≤ODs ≤4 ×ODc, and strong producers by ODs >4 ×ODc. ODc was the OD of the negative control, while ODs were the OD of the tested samples (Stepanović *et al*., 2007).

Molecular identification of the selected bacterial isolate

The selected *P. aeruginosa* isolate P21 was identified

molecularly by amplification and sequencing of the *16S rRNA* gene using polymerase chain reaction (PCR). A thermal cycler (ABI 2720) was employed to amplify the gene using two primers; F: 5'-GGGGGATCTTCGGACCTCA-3' and R: 5'-TCCTTAGAGTGCCCACCCG-3' (Tripathi *et al*., 2013). The genomic DNA was observed on an agarose gel at a concentration of 0.8%. The sequencing was carried out utilizing the Big Dye Terminator Cycle Sequencing Kit according to the manufacturer's instructions, and the data was assessed using V. 3.1, Applied Biosystems analyzer. Finally, the 16S rDNA sequencing for isolate P21 was submitted to the NCBI GenBank database and assigned an accession number (Kumar *et al*., 2016).

Phage enrichment, purification, and amplification

A phages was isolated from wastewater collected from Abo ELalazium Hospital, Cairo, Egypt. Initially, wastewater was mixed with culture of the Ps21 isolate and incubated at 37 C. .After 24 h of incubation, the sample was centrifuged at 4°C for 15 min at 5000 rpm. Chloroform 1% was used to lyse the bacteria that contained the phages. Furthermore, to remove bacterial debris, the sample was filtered through 0.2 µm syringe filters (Ismael *et al*., 2024). To determine the inhibition activity of the isolated phages against the selected bacterial host (Ps 21 strain), a spot assay was conducted on the lawn of the host strain. After incubation for 24 h, the phage's lysis activity was assessed depending on its apparent clarity. To purify the phage, the clear lysis plaques were cut off from the agar using a micropipette tip and placed in sterile SM buffer (pH 7.5). The isolated phage was centrifuged at 7000 rpm and 4°C for 15 min. Following performing a ten-fold serial dilution, the supernatant was spotted onto the new lawn of the host strain Ps 21. The purification methods were performed six times to verify high purity of the phage (Echeverría-Vega *et al*., 2019). Phage amplification was performed in a broth culture of TSB, followed by cold centrifugation at 5000 rpm for 15 min, and finally collection of the supernatant was performed. The phage quantity was determined by conducting a ten-fold serial dilution and applying 10 µL of every dilution on a new lawn of the host strain Ps 21. The isolated phage was preserved in SM buffer at pH 7.5 (Fayez *et al*., 2023).

Morphological characterization of the phage using transmission electron microscopy (TEM)

The morphology of the *Seudomonas* phage was studied *via* transmission electron microscopy (TEM) (JOEL-JEM- 1010 electron microscope operated at 80 KV, Japan) One drop of the isolated phage suspension (10^{10} pfu/ml) was placed on a copper grid coated with 200 mesh carbons, and allowed for absorption for about 20 min. before an extra liquid was eliminated using a filter paper. The grid was stained with 2% uranyl acetate (pH 4.5) for 90 sec, allowed to dry, and analyzed using a JOEL-JEM-1010 TEM at 80 KV (Liu *et al*., 2022).

Host range determination

To assess the phage host range, 35 *P. aeruginosa* bacterial isolates were evaluated using the spot testing approach described by Kutter (2009). Briefly, 100 µl of freshly prepared bacterial culture were added to a tube containing 4 ml semi-solid tryptic soya agar medium. Tube contents were poured into a plate of tryptic soya agar medium. One drop (10 µl) of the phage was spotted onto the surface of bacterial lawns. Following an overnight incubation, the plates were studied, and the plaques were evaluated based on their apparent clarity.

Relative efficiency of plating (EOP)

The efficiency-of-plating method (EOP) was applied to further assess phage efficacy against *P. aeruginosa* host strains. In brief, a phage stock was tenfold diluted (10^{1} to 10^{8}). 10 µl of each dilution were spotted in triplicate on a new lawn of each sensitive bacterial isolate identified using the host range assay. Following an overnight incubation, each bacterial isolate's average plaque-forming unit (PFU) was calculated (Kutter, 2009). The relative EOP was determined by dividing the average PFU count of the phage on each bacterial host by the highest PFU value measured. The EOP value was classed into four groups; mainly "Low production" if the ratio was between 0.001 and 0.1, "Medium production" if the EOP was 0.1 or higher but less than 0.5, and "High production" if the ratio was 0.5 or higher. An EOP equal to or less than 0.001 was deemed inefficient (Mirzaei and Nilsson, 2015).

Optimal multiplicity of infection (MOI) assay

Multiplicity of infection (MOI) is defined as the number of viral particles/ number of host cells. To calculate it, the total number of used infectious viral particles was divided by the total number of bacterial cells in a culture. *P. aeruginosa* was grown overnight in fresh TSB and mixed with the stock phage at various MOI ratios including 0.001, 0.01, 0.1, 1.0, 10, and

100. The mixtures were shaker incubated at 120 rpm for 5 h at 37 °C. After incubation, the phage samples were centrifuged at 6000 rpm for 20 min at 4 °C. The supernatants were filtered using 0.22 µm membranes. The phage titer in the resulting supernatant was determined with a double-layer agar plate technique. In this technique decimal dilutions of the phage lysate were performed using saline solution as diluent from 10^{-1} to 10^{-10}, then 100 µL of each dilution of phage were added to 100 µL of the host culture in a tube containing 4 ml of melted semi-solid tryptic soya agar. The mixture was poured onto a plate containing the base layer of TSA and incubated for 24 h at 37°C. The presence of plaques was detected after incubation of the plates. Plaques were counted and titer of phage was recorded as plaque forming units/ ml (PFU/ml) as the following: Titer = number of plaques × dilution factor × 100)/ volume plated (µL) (Zaki *et al*., 2023). The optimal MOI was that yielded the highest final phage count (PFU/mL) (Liu *et al*., 2024).

Adsorption assay

An adsorption assay was used to determine how long it took the *Pseudomonas* phage to cling to the bacterial host. In a tube, 10 ml of *P. aeruginosa* at MOI 0.01 were mixed with 100 µl of *Pseudomonas* phage solution. An aliquot (100 µL) was withdrawn at 0, 2, 3, 5, 7, 10, 12, and 14 min intervals and centrifuged for 1 min. at 10,000 rpm. Afterward, ten-fold serial dilutions were applied and the phage was detected on double-layer agar containing the host bacteria (Rombouts *et al*., 2016).

One-step growth curve

The phages' burst sizes and latent periods were assessed using a one-step growth assay, as reported by Merabishvili *et al*. (2014), with slight modifications. At an MOI of 0.1, the phage and *P. aeruginosa* were incubated at 37 °C and shaken at 150 rpm. A sample (1 ml) was withdrawn every 5 min for more than 1 h. Afterward, the mixture was titrated every 5 min using a double-layer agar plate. The latent period was evaluated as the duration of time after infection where additional phage progenies particles were developed. The relative burst size was estimated as the ratio of the titer of released virions at plateau to the initial virions titer (Zaki *et al*., 2023).

Phage physicochemical and storage stability

The stability of the *Pseudomonas* phage was examined by subjecting the phage suspensions to various environmental conditions and evaluating residual phage titers via spotting on double-layer agar plates containing the host bacterium. First, the phage was exposed to different temperatures of 4, 25, 37, 40, 50, 60, 70, 80, and 90 °C for 1 h each. Second, its stability was tested through subjecting it to a pH ranging from 3 to 12 for 1 h each. Finally, the phage was also subjected to UV radiation at durations of 0, 15, 30, 45, and 60 min using a disinfectant UV lamp (~260 nm) (Kropinski *et al*., 2009). For six months, RM_Ps3 phage was stored at -20, 4, and 28 °C in SM buffer. When the phage was held at −20 °C, glycerol (30%) was added to the phage as a protectant. The double-layer agar method was used to measure the phage titer each month (Xu *et al*., 2023). Three duplicate of each experiment were conducted.

In vitro antibacterial activity of Pseudomonas phage

Pseudomonas phage at various MOIs (*i.e.,* 0.001, 0.001, 0.01, 0.1, 1, 10, and 100) was grown with the host bacterium (Ps 21) to determine the phage's ability to eliminate bacterial growth *in vitro*. In a 96-well microplate, 180 µl of bacterial suspension (10^6 CFU/mL) were combined with 20 µl of phage at different titers (10^4 to 10^9 PFU/mL) to obtain different MOIs of 0.001, 0.001, 0.01, 0.1, 1, 10, and 100. The microplate was incubated at 37 °C, and data was collected using a microplate reader (FLUOstar Omega, BMG LABTECH, Ortenberg, Germany) at 600 nm every 30 min. for 9 h (Chen *et al*., 2018). Untreated bacterium was used as control. The percentage of OD_{600} reduction after 9 h of incubation was estimated using the following formula reported by Abdelrahman *et al*. (2025):

$$\textit{Percentage (\%) of in vitro reduction} = \Delta OD_{600} \textit{ of treated sample/ the control's starting } OD_{600} \times 100$$

Bacteriophage potency against bacterial biofilm's production

At various MOIs (*i.e.*, 100, 10, 1, 0.1, 0.01, and 0.001), the phage's anti-biofilm activity was assessed for two distinct phenotypes: (i) biofilm formation inhibition and (ii) biofilm clearing. With a few minor adjustments, the 96-well microtiter plate was used for biofilm formation, staining, and quantification. Approximately, 180 µL of the bacterial strain Ps21 suspension (10^6 CFU/mL) were inoculated into the plate. An untreated culture served as a negative control (Merritt *et al*., 2011).

Biofilm formation inhibition assay

The antibiofilm ability of the phage was evaluated with various multiplicities of infections (0.001 to 100) with a total volume of 20 µl of a phage. From the beginning of the experiment, a bacterial culture was exposed to phage infection. They further incubated for 48 h at 37˚C without shaking before being stained with crystal violet. Every MOI was assessed in six replicate (Merritt *et al*., 2011).

Biofilm clearance assay

The biofilm clearing process was the same procedure as the inhibition biofilm formation assay, with the difference of allowing all cultured bacteria to produce mature biofilms in the wells for 48 h. The different MOIs of the phage were subsequently introduced to the plate's wells, which contained the bacterial culture, and incubated for another 24 h at 37˚C. The culture medium and planktonic bacteria were disposed of and then the plate was washed with distilled water. After drying and dumping the plate, 150 µL of newly made 0.1% crystal violet (CV) were used to dye the adhering biofilms. Plates were cleaned again and allowed to dry at room temperature, with any extra crystal violet disposed of. Then, 150 µL of 30% acetic acid solution were used to dissolve those pigmented biofilms. The optical density was determined by measuring the absorption of solubilized dyed biofilm formed at 595 nm using the FLUOstar Omega Microplate reader (BMG LABTECH, Germany) (Zaki *et al*., 2023). The percentage (%) of inhibition and eradication was calculated according to the following equation (Kamer *et al*., 2023):

$$Percentage\ of\ inhibition/\ Eradication\ (\%) = [(OD_{Untreated} - OD_{Treated})/\ OD_{Untreated}] \times 100$$

Statistical analysis

Three duplicate of each experiment were conducted, and the mean±standard deviation (SD) was used to express the results. The software GraphPad Prism 10.5.0 was used for data analysis and graph generation using one-way ANOVA.

Results

Identification of the clinical isolates

This investigation comprised 35 *P. aeruginosa* isolates that were obtained from 47 different clinical samples, such as swabs from wound infections (14 isolates), blood (10 isolates), urine (7 isolates), and sputum (4 isolates). The obtained clinical isolates displayed pink colonies on MacConkey agar as shown in Figure 1A, and bright blue-green coloration on cetrimide agar (Figure 1B). The biochemical Vitek-2 method confirmed their identity as *P. aeruginosa* with 99% confidence.

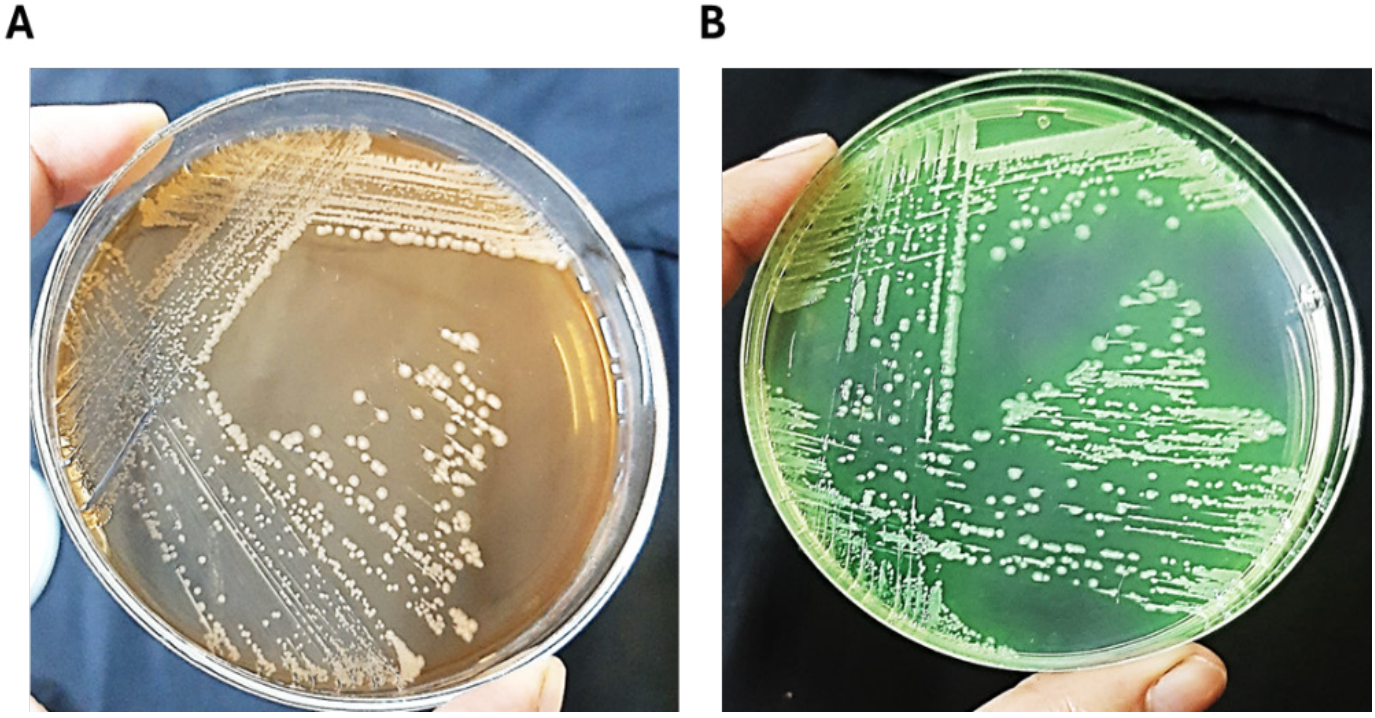

Figure 1: *Phenotypic morphology of P. aeruginosa isolates grown on (A) MacConkey agar; (B) Cetrimide agar after 24 h of incubation at 37 °C.*

Phenotypic and genotypic resistance patterns of P. aeruginosa isolates

A Vitek-2 device was utilized to assess the susceptibility profile of *P. aeruginosa* strains against several antibiotics. CLSI standards were followed for the interpretation of the results. Different drugs showed different sensitivity responses against *P. aeruginosa* isolates. The data indicated that meropenem, imipenem, and ticarcillin-clavulanate were inefficient (0% inhibition) over all tested isolates. However, the isolates showed resistance to tobramycin and ceftazidime (94% each), piperacillin-tazobactam (86%), gentamicin and ticarcillin (80%), piperacillin (71%), ciprofloxacin (67%) cefepime (66%), amikacin (51%). On the other hand, all isolates of *P. aeruginosa* were sensitive to colistin (100%). The obtained results of bacterial susceptibility to various antibiotics (13 items) revealed that all isolates exhibited multiple-drugresistance (MDR). Individual bacterial isolates MDR calculations showed that *P. aeruginosa* Ps21 had the highest MDR value (0.94). The study area was categorized as a potentially health-risk environment revealed by obtaining MDR index values above 0.25, as shown in Figure 2. Hence, Ps21 isolate; a carbapenem-resistant representative isolate, was selected for resistance genes detection. The Biofire Film Array Panel was used to examine the clinical blood sample of isolate Ps21, allowing for quick detection of the of antimicrobial resistance genes. According to the obtained results, the selected *P. aeruginosa* isolate (Ps21) carried the *blaNDM* gene, which was considered as a sign of resistance to carbapenem antibiotic.

Evaluation of the biofilm development by isolates of P. aeruginosa

Pseudomonas aeruginosa isolates' ability to form biofilms was evaluated spectrophotometrically using the crystal violet assay. According to their capacity to form biofilms, the isolated bacteria were divided into three groups (Figure 2): Strong biofilm-formers (60 %), moderate biofilm-formers (20 %), and weak biofilm-formers (20 %).

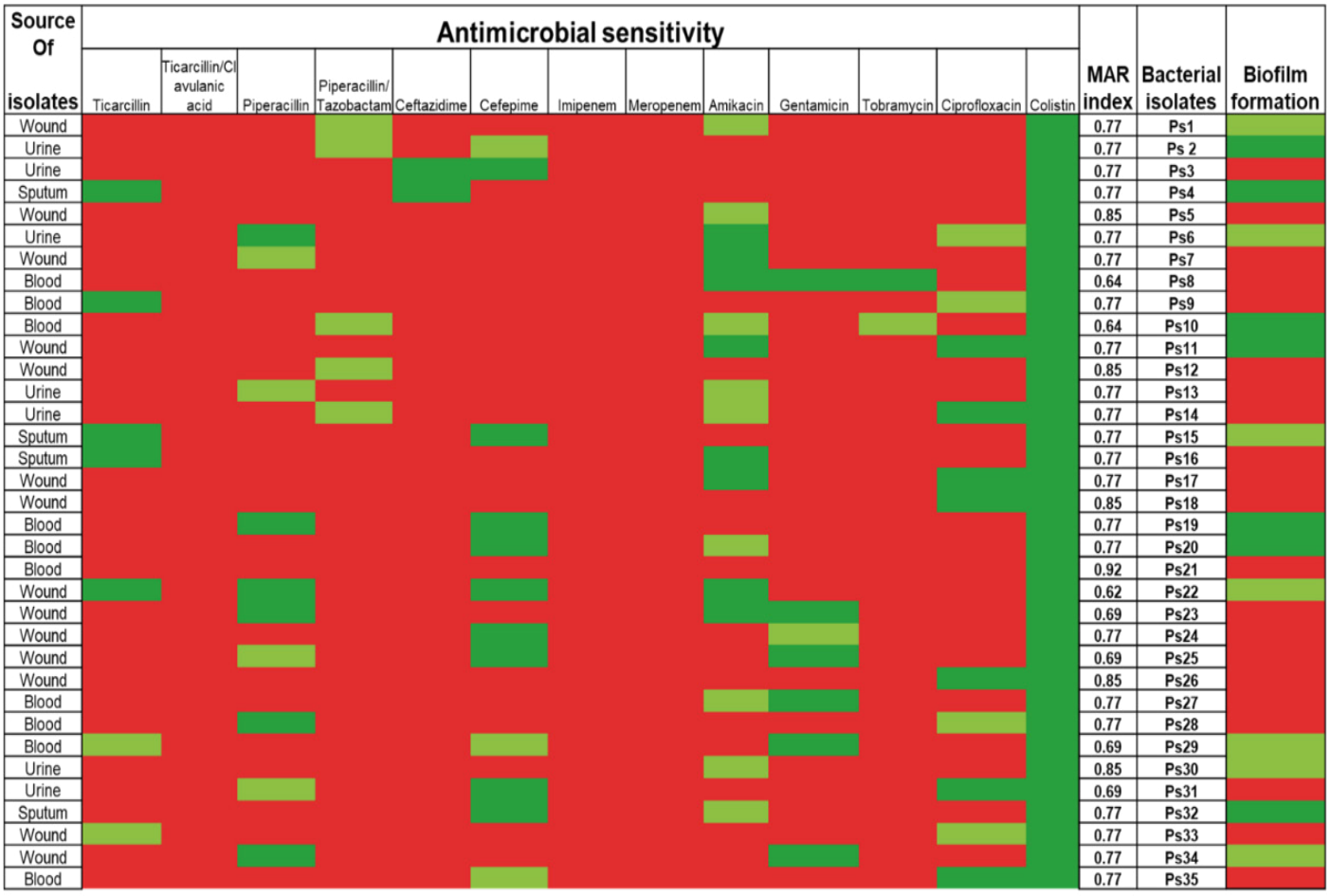

Figure 2: *A heatmap of the antimicrobial profile of the P. aeruginosa isolates against 13 antibiotics; where resistant is indicated in red color, intermediate in light green, and sensitive in dark green. Biofilm formation are indicated (strong formation indicated in red, moderate in light green, and weak in dark green) and MAR index values.*

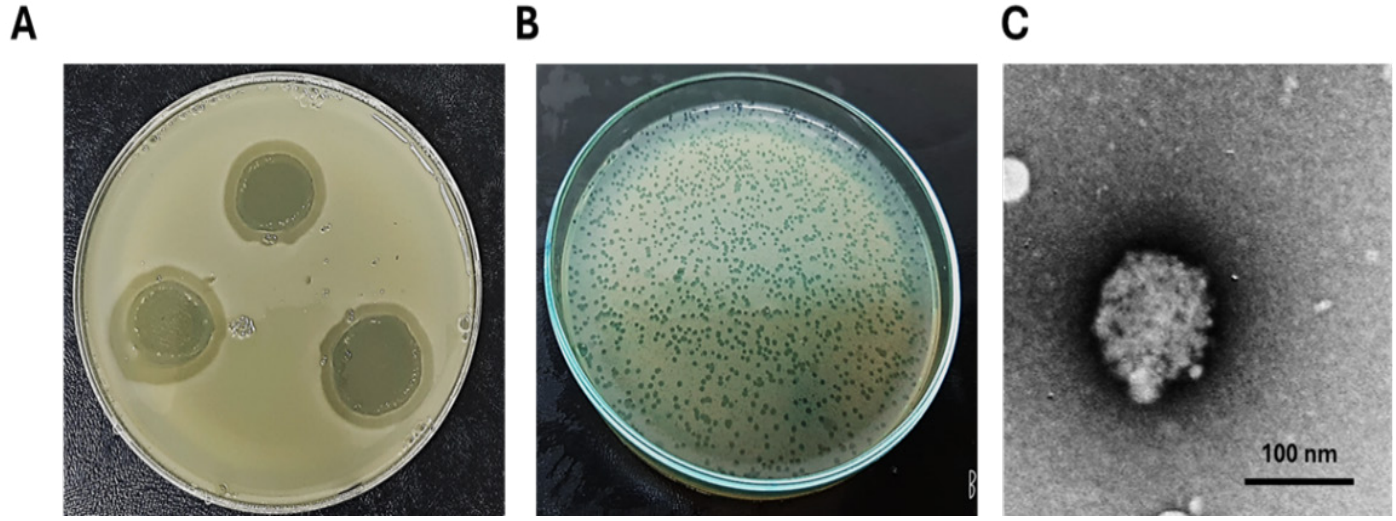

Figure 3: *Isolation of bacteriophage. (A) Clear lytic zones on bacterial lawn observed using spot test of phage lysate from sewage. (B) Plaque morphology of isolated phage using double layer agar plate. (C) Transmission electron microscope (TEM) images of RM_Ps3 phage (Phage particles were negatively stained with 2% phosphotungstic acid. Scale bar = 100 nm).*

Molecular identification of the selected P. aeruginosa strain

The representative isolate *(P. aeruginosa*, Ps 21) was selected for further identification *via 16 S rRNA* gene amplification and sequencing. After PCR amplification, 2% agarose gel electrophoresis was performed which yielded a single, unique fragment with a molecular weight of 1166 bp. An accession number of PV094177 was assigned to the nucleotide sequences after being uploaded on the NCBI GenBank database in the United States.

Phage morphological characterization by TEM

Using the spot assay, the *P. aeruginosa* phage RM_Ps3 created a clear lytic zone on the bacterial lawn (Figure 3A), and the double layer agar approach produced 1 mm-diameter circular plaques (Figure 3B). According to the TEM image, the RM_Ps3 phage was closely linked to phages of the Podoviral morphotype in the order Caudovirales, with a short, non-contractile tail length of 17.8 nm, and an icosahedral head diameter of 60 nm (Figure 3C).

Estimating the phage host range and relative plating efficiency

Clear zones; a sign of bacterial lysis, were observed in the spotting region of Phage RM_Ps3 against various antibiotic-resistant bacterial strains. Of the 35 *P. aeruginosa* isolates that were examined, 30 were lysed by phage RM_Ps3. According to the obtained data, phage RM_Ps3 expressed lytic activity against 86% of the tested clinical isolates of *P. aeruginosa*, indicating a broad host range (Figure 4A). Relative EOP analysis was used to further assess the lytic capacity and pathogenicity of phage RM_Ps3 (Figure 4B). The indicator host used for determining the relative EOP was the selected bacterial isolate Ps21, since it produced the highest phage titer. 6 strains out of 30 *P. aeruginosa* isolates that were antibiotic sensitive had high EOP, 19 isolates had medium EOP, and 5 isolates had low EOP.

The one-step growth curve, adsorption rate, and optimal MOI

The ideal MOI test's results, which involved infection with *P. aeruginosa* at different MOIs, indicated that the maximal phage titer (10^{10} PFU/mL) was achieved successfully at an MOI of 1. After that, phages with MOIs of 0.1, 0.01, and 0.001 exerted greater efficacy compared to those with MOIs of 10 and 100 (Figure 5A). A line graph showing the percentage of unadsorbed phages over a certain period of time was created from the obtained results of the adsorption rate assay. The phages were completely adsorbed by *P. aeruginosa* around 10 min. after treatment, suggesting a rapid rate of adsorption (Figure 5B). The one-step growth test conducted at MOI 0.1 was used to measure the latent time and burst size. The latent period was around 15 min., according to the curve. It took 25 min. to complete the process from adsorption to the release, because the preparation required 10 min. as well. Moreover, Figure 5C demonstrates that for every bacterial cell, the burst size was approximately 300 phages.

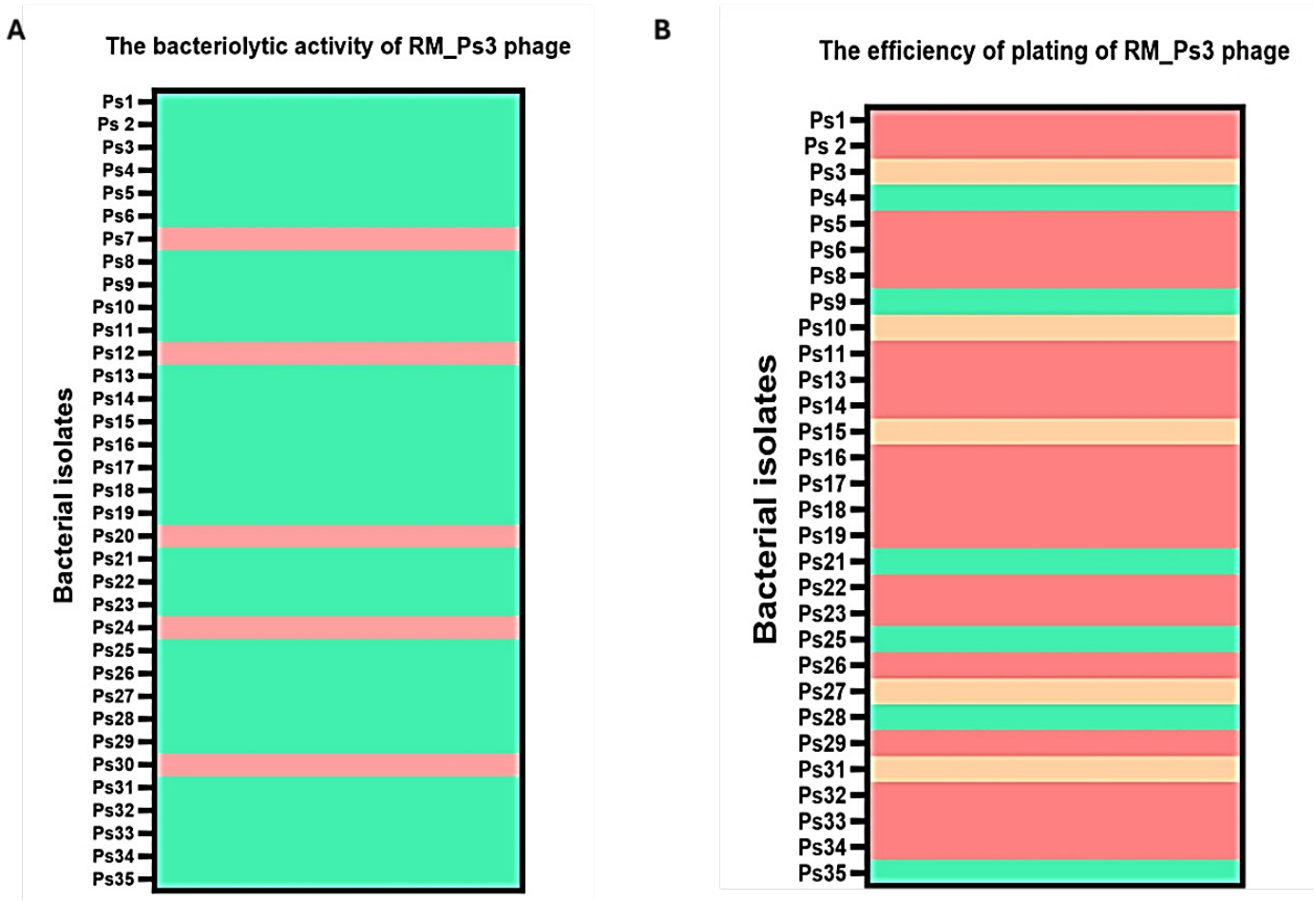

Figure 4: *Heatmap of host range and EOP for different P. aeruginosa isolates tested against Pseudomonas phage (A) The host range results are represent by green for lysed bacteria and red for resistant bacteria. (B) The EOP values represented as green (≥ 1), red (≥ 0.001 and < 1), and orange (< 0.001).*

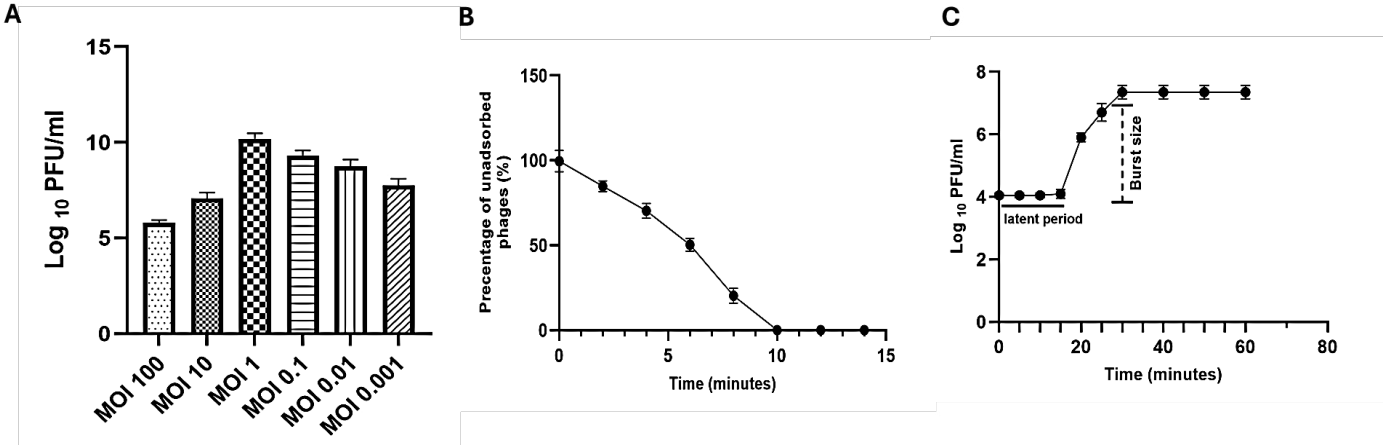

Figure 5: *The activity of a Pseudomonas RM_Ps3 phage against the host bacterium. (A): The phage titer after 5 h of incubation with different MOIs, (B): The adsorption curve demonstrating the adsorption percentage over time, and (C): The one-step growth curve of the phage.*

Phage's physical and storage stability

Through observation of the changes in phage titer during incubation at several temperatures, the thermal stability of RM_Ps3 was evaluated. According to the findings, the phage RM_Ps3 tolerated a broad range of temperatures. The isolated phage slightly decreased ($P < 0.05$) its titer at a temperature of 60 °C. However, Figure 6A illustrates that the phage titer was considerably reduced ($P < 0.0001$) when the RM_Ps3 phage was incubated at higher temperatures such as 70, 80, 90, and 100 °C. The ideal pH stability range for phage RM_Ps3 was 3.0–12.0, where it preserved

an outstanding activity without lowering the phage titer. But when subjected to severe pH value of 12.0, it stopped working (Figure 6B). When exposed to UV light, the phage titer progressively dropped (P < 0.0001) over duration of 45 min. After 15 min, there was a 3 $\log_{10}$ PFU/mL drop, and after 30 min, there was another 3 $\log_{10}$ PFU/mL drop. Finally at 45 min, there was a total inactivation (P < 0.0001) (Figure 6C). For six month, the phage was kept at -20, 4, and 28 °C and its titer was checked each month. Phage titer that was kept in SM buffer at 4°C did not decrease over the course of six month, while these kept in glycerol 30% at -20°C was slightly decreased. In contrast, phage titer kept in SM buffer at 28°C rapidly decreased with time demonstrating that 4°C was an appropriate temperature for RM_Ps3 phage storage (Figure 6D).

Antibacterial activity

The optical density (OD_{600}) of the untreated bacteria increased, while the phage RM_Ps3 was cultured coupled with its host over various MOIs (100, 10, 1, 0.1, 0.01, and 0.001) within the first 7 h exhibited almost no change in OD value. Following this, the OD of the bacteria treated with different MOIs rose again, but more than that of the bacteria treated with a low MOI. The bacteria treated with MOI 100 displayed the greatest rise, whereas those bacteria treated with MOI 1 expressed the least increase. This showed that the RM_Ps3 phage effectively controlled the growth of its host at various MOIs as shown in Figure 7A. The percentage of OD reduction after 9 h of incubation was calculated (Figure 7B). The results obtained showed that all MOIs considerably reduced (P < 0.0001) bacterial growth, compared to untreated bacteria. Phage with MOI values of 10, 1, 0.1, and 0.01 represented the most effective MOI in preventing bacterial growth (*i.e.*, no discernible turbidity) during the incubation period, as shown in Figure 7C.

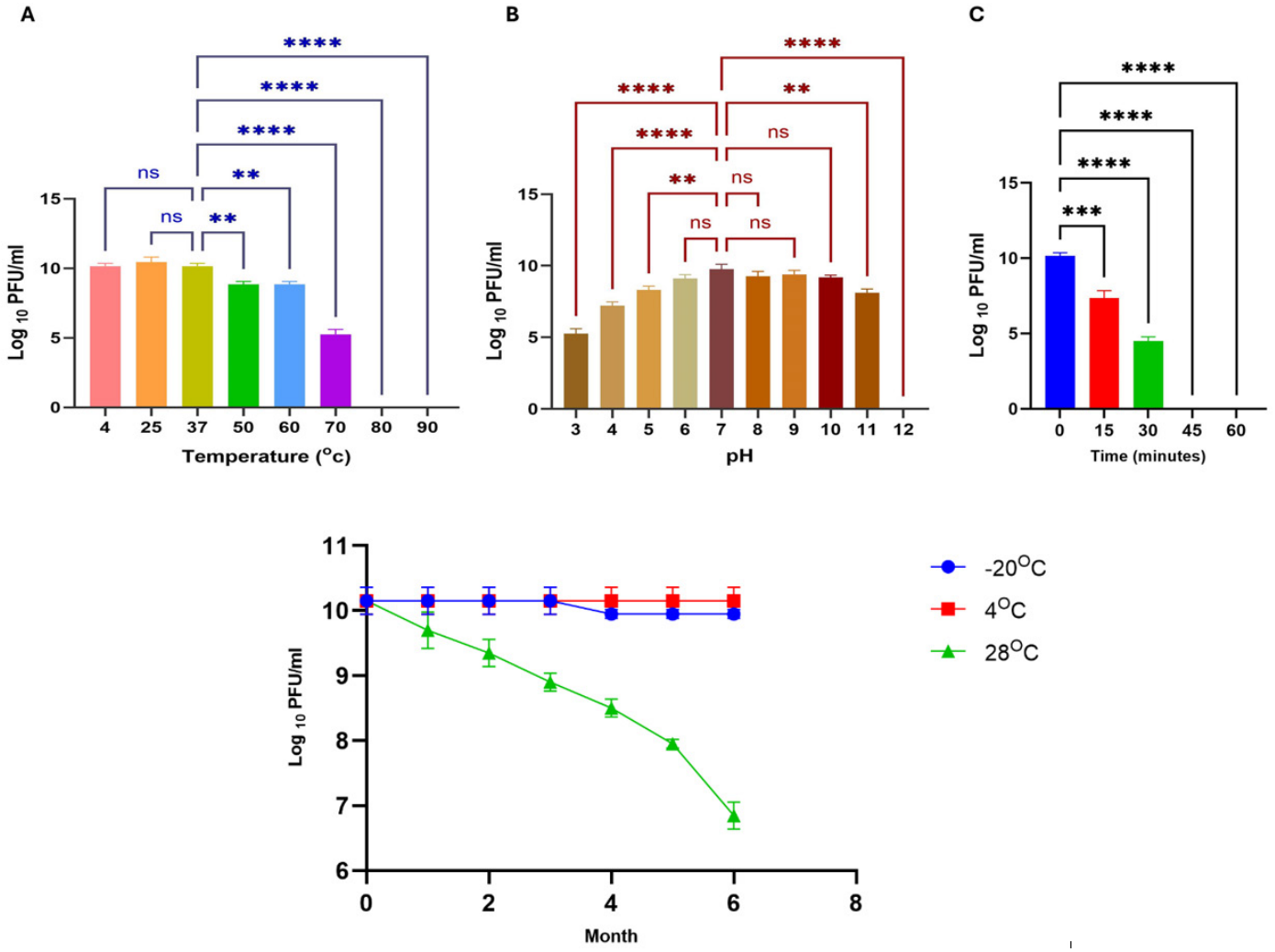

Figure 6: *Phage stability at different ranges of temperatures (A), pH (B), UV exposure (C), and storage stability of phages at -20, 4 and 28 °C within 6 month (D). PFU: Plaque forming unit. Data is displayed as mean ± SD. Statistically significant differences are marked by asterisks, where **indicates (P < 0.05), ****indicates (P < 0.0001), and ns indicates non-significant difference (P ≥ 0.05).*

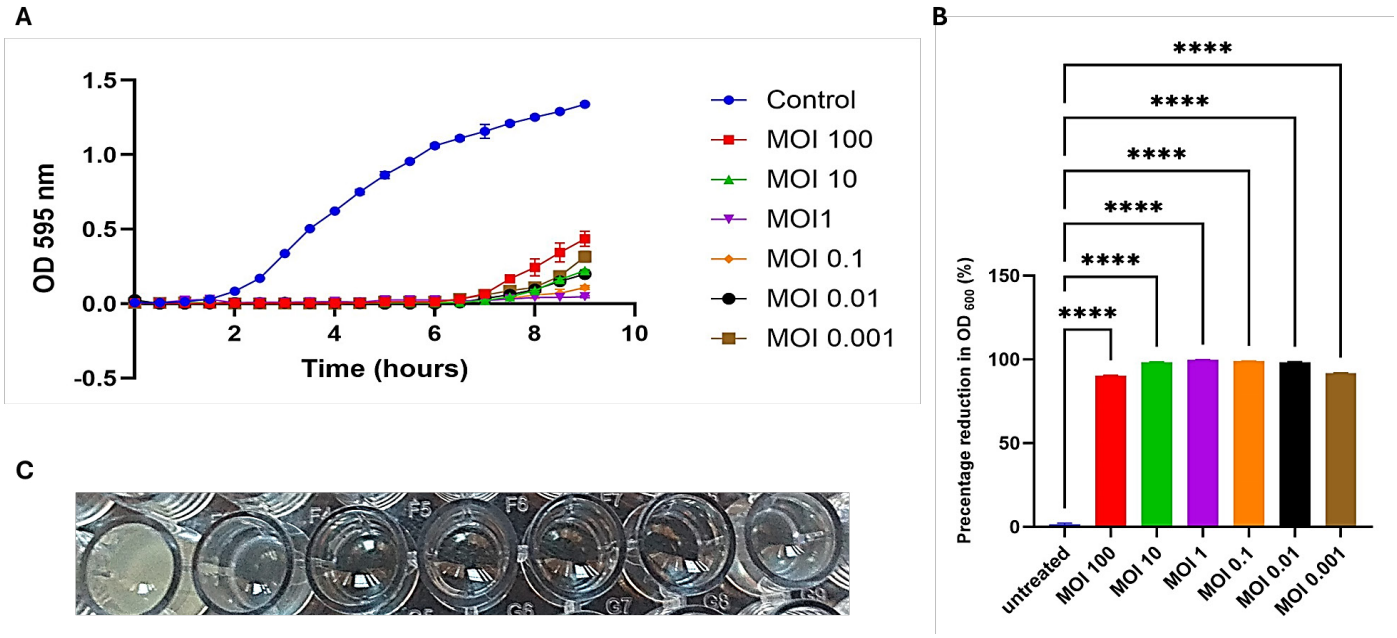

Figure 7: *Kinetics of the RM_Ps3 phage interaction against P. aeruginosa P21 at 37 °C. The bacterial growth (OD_{600}) of untreated P. aeruginosa (control) and bacteria treated with phage RM_Ps3 at various MOIs (0.001, 0.01, 0.1, 1, 10, and 100) over a 9-h period is displayed in (A) time-killing curve. (B) The percentage decrease in OD_{600} for bacteria treated with phage RM_Ps3 at various MOIs following 9 h of incubation. (C) The 96- well plate showing different MOIs that prevented the detection of bacterial growth, compared to the control. Data is displayed as mean ± SD. The data is statistically significant considering P < 0.0001 (****).*

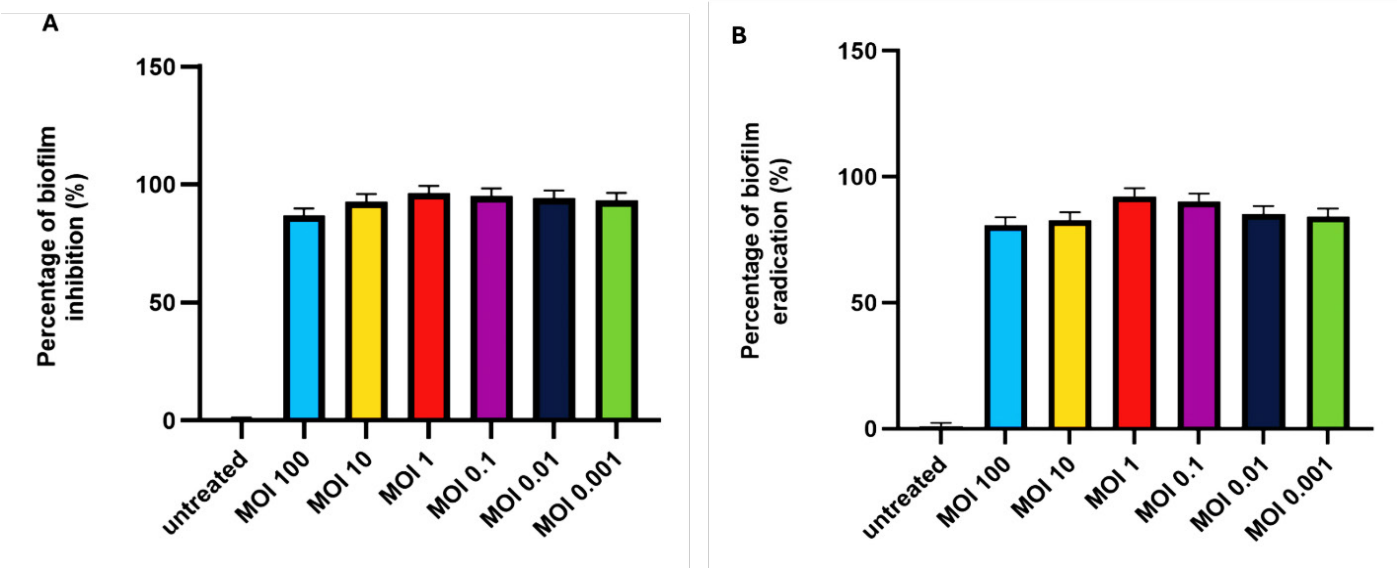

Figure 8: *Antibiofilm activity of RM_Ps3 phage against P. aerugionosa P21. (A): Phage inhibition of biofilms formation at different MOIs after 48 h of incubation in 96-well plates. (B): Phage degradation of mature biofilms at different MOIs after 72 h of incubation in in 96-well plates. Data is displayed as mean ± SD.*

Antibiofilm potential (inhibition and clearance)

Phage RM_Ps3's antibiofilm activity was evaluated *via* experiments carried out at a variety of MOIs. Evaluations were made of both, removal of a biofilm and inhibition of biofilm development. A calculation of the percentage (%) of inhibition revealed that the highest percentage (96%) was detected at an MOI of 1, followed by 95% at an MOI of 0.1, 94% at an MOI of 0.01, 93% at an MOI of 0.001, and 92% at an MOI of 10. The lowest percentage of 87% was detected at an MOI of 100. Bacterial biofilm growth was appreciably reduced at all evaluated MOIs following 48 h incubation, compared to the untreated culture (Figure 8A). The results of calculating the percentage (%) of eradication showed that the highest percentage (92%) was detected at an MOI of 1, followed by 90%

at an MOI of 0.1, 85% at an MOI of 0.01, 84% at an MOI of 0.001, and 82% at an MOI of 10. The lowest percentage (80%) was detected at an MOI of 100. At MOI 1, the strongest antibiofilm was detected. The efficacy of phage RM_Ps3's invasion was demonstrated by evaluating its capacity to degrade mature biofilm. A mature biofilm treated with various MOIs was successfully broken up after 48 h for all treated cultures, as demonstrated by the fact that their ODs were much lower than those of the untreated mature biofilms (Figure 8B). The best antibiofilm potential was demonstrated by phage RM_Ps3 at 1 MOI, where it destroyed the mature biofilms and prevented the formation of new biofilms.

Discussion

Pseudomonas aeruginosa; an antibiotic-resistant bacterium belonging to the ESKAPE group is a major threat to world health and is the causative agent of the majority of severe infections, including pneumonia, lung and urinary tract infections (Litwin *et al*., 2021). These were attributed to the widespread usage of antibiotics and the continuing rise of antibiotic resistance. Therefore, finding alternate antibacterial methods is crucial. Phage therapy is showing promise as a treatment option. Despite being utilized almost a century ago, phage therapy lost its attraction as treatments with antibiotics are widely available. However, phage therapy has regained international attention due to the present challenge of the rise in antibiotic resistance Pires *et al*. (2017).

Initially, *P. aeruginosa* isolates resistant to carbapenem were isolated to check for phage susceptibility. Finding MDR *P. aeruginosa* isolates was fortunately not difficult. Next, the RM_Ps3 phage was selected, described, and its lytic efficiency against *P. aeruginosa* isolates that were resistant to carbapenem was evaluated. Using the Vitek 2 approach, 31 isolates of *P. aeruginosa* were identified, which were collected from Egyptian hospitalized individuals. Following that, the Vitek 2 AST system was utilized to test for antibiotic sensitivity of these isolates using 13 distinct antibiotics. All the tested isolates showed phenotypic resistance to carbapenems. Compared to earlier studies conducted in Egypt by Khalifa *et al*. (2019), Abdelaziz *et al*. (2021), this rate was alarmingly higher. Since carbapenem is mostly used as a last resort to treat multi-drug resistant infections; thus, resistance to antibiotics is a serious problem. These obtained results are in line with the results reported by Afify *et al*. (2024) who found that 98.2% of the examined isolates exhibited phenotypic resistance to carbapenems. With a MAR index > 0.62, each bacterial isolate displayed a highly resistant phenotype. According to the isolates' MAR indices, they were collected from locations where resistant bacteria were highly prevalent, potentially because of antibiotic abuse. They displayed resistance to remarkable antibiotic classes in their antimicrobial profiles. Worldwide, nosocomial diseases were linked to *P. aeruginosa* which rapidly developed antibiotic resistance through several pathways (Davis and Brown, 2016). By employing a Bio fire film array, a genotypic screening for the genes that encode for carbapenemase was additionally conducted. The results obtained showed the presence of *blaNDM* gene. This result is consistent with a study conducted in Egypt by Basha *et al*. (2020), which revealed that the most common carbapenemase-encoding gene among the carbapenem resistant *P. aeruginosa* was *blaNDM*.

Additionally, biofilm are believed to have a key role in preventing patient's recovery resulting in chronic infections. The prevention of chronic and persistent infections depends on the identification of biofilms formation and the assessment of therapeutic activity of the various medications (Kırmusaoğlu, 2016). The quantitative microtiter plate (MTP) method was employed in this study to detect the formation of biofilms, and the obtained results showed that all isolates generated biofilms with varying degrees. Strong biofilms were formed by about 60% of the analyzed *P. aeruginosa* isolates, moderate biofilms by 20%, and weak biofilms by 20%. These findings are consistent with those of Hemmati *et al*. (2024), who reported that 99.0% of *P. aeruginosa* isolates were found to be biofilm producers, where 46.2% of these isolates with MDR patterns were strong producers, while 34.9% and 17.9% had moderate and weak biofilm patterns, respectively. According to a previous study, biofilm formation is one of the factors contributing to *P. aeruginosa* infection recurrence, which may pose serious treatment difficulties for hospitalized patients (Qin *et al*., 2022). So, phage therapy is used as alternative therapeutic agent to treat these infections caused by carbapenem-resistant *P. aeruginosa* (Chegini *et al*., 2020). Ps21 isolate was selected for phage isolation and additional studies since it generated the strongest biofilms formation ability with the highest recorded MAR index value.

According to the antibiotic profile and biofilm formation, the representative isolate, Ps21, was further identified by amplifying and sequencing of its 16S rRNA gene. The nucleotide sequence assigned an accession number of PV094177 to this isolate upon being uploaded to the NCBI GenBank database in the Unitd States.

Hence, phage therapy could represent a viable substitute approach to manage the problematic rise in *P. aeruginosa* antibiotic resistance. Bacteriophages are considered to be safer, better tolerated, and not harmful to mammalian cells, compared to the antibiotics (Kakasis and Panitsa, 2019). Additionally, there is no need to administer phage dosages repeatedly as the case with antibiotics. After just one dosage of phages, auto "dosing" causes a considerable rise in phage concentration at the infection site, leading to increased bacterial death (Abedon and Thomas-Abedon, 2010).

Numerous studies indicated that the best sites for phage isolation, which impact harmful bacteria are wastewater sources (Alharbi and Ziadi, 2021; Aghaee *et al*., 2021; Marashi *et al*., 2022). Finding the right locations for phage isolation will increase their cost-effectiveness by decreasing time. In this investigation, particular phages of the host strain were isolated from the hospital wastewater source associated with the host strain.

In the present work, TEM results demonstrated that RM_Ps3 phage had a short, non-contractile tail and an icosahedral head. It belonged to the podoviral morphotype within the Caudovirales order. In accordance with our results, the podoviral and myoviral morphotype phages have been proven to be crucial and are strongly recommended for phage therapy (Alemayehu *et al*., 2012).

According to Fong *et al*. (2021), the host range and EOP evaluation outcomes are crucial factors that must be taken into consideration during the selection of bacteriophages for therapeutic applications. With a wide host range, the phage RM_Ps3 was able to lyse 30 of the tested 35 (86%) *P. aeruginosa* isolates Traditional antibiotics used to treat *P. aeruginosa* infections were not effective against the majority of these strains. However, broad host range phages are recognized as be more effective for biocontrol and preferred for therapeutic usage in phage therapy (Venkataraman *et al*., 2025).

Upon using phage therapy, the burst size and latent duration should be prioritized. Phages that have big burst sizes and short latent periods are frequently better for lysing bacteria (Zhu *et al*., 2025). In this study, RM_Ps3 showed both a short adsorption rate and a short latent duration. For each infected cell, the RM_Ps3 phage displayed a huge burst size of about 300 PFU. This is consistent with the findings obtained by Wannasrichan *et al*. (2022), which demonstrated that Phage JJ01 needed at least 10 min. for 90% of its particles to be adsorbed to the host cells and had a latent period of 30 min. inside the host cell for multiplication. The bursting size of JJ01 was comparatively large. According to this study analysis, the optimal MOI needed for phage amplification was 1, in accordance with Wei *et al*. (2025) findings, which revealed that the maximum titer of phage HJ01 was released at a MOI of 1, suggesting that this was the optimum MOI for phage HJ01.

Phage RM_Ps3 also expressed greater stability throughout a broad range of pH, UV, and temperature. It is essential to evaluate the stability of a phage under different pH and temperature ranges to provide information about its application and storage. For therapeutic uses, phages should be strong in extreme environments to withstand the unfavorable environmental changes (Akremi *et al*. 2022). The obtained results are in agreement with those of Zhang *et al*. (2024), who isolated two phages that show good resistance to temperature and acidic/alkaline conditions, beneficial for their use and storage. Additionally, our study showed that the RM_Ps3 phage when exposed to UV light gradually becomes inactive, reaching full inactivation within 45 minutes. These results are consistent with those of a prior study conducted by Mohamed *et al*. (2025), revealing that phage vB_Ps_ZCPS13 became totally inactive after 45 minutes of UV exposure.

One of the most important factors in turning biopharmaceuticals into commercial medicinal products is long-term storage stability, because the company incurs more costs when phage products need to be refreshed frequently (Dini and de Urraza, 2013). This study demonstrated that RM_Ps3 phage in SM buffer maintained its titer without changing for 6 month at 4 °C. These findings are consistent with those of Xu *et al*. (2023), who found that phage titers

varied between 1 × 10^{10} PFU/ml and 5 × 10^{10} PFU/ml but did not decrease within 12 months when the phage was stored in SM buffer at 4 ˚C, suggesting that 4 ˚C was an appropriate temperature for phage storage. But within a year at 28 ˚C, the phage titers drastically decreased by more than eight orders of magnitude, making the phage useless.

The therapeutic efficacy of phage RM_Ps3 was assessed by incubating it with the host bacterium at various multiplicities of infections (MOIs). During the first 7 h of the experiment, all MOIs displayed greater effectiveness against the tested bacteria, compared to the untreated ones, which proliferated steadily. Beginning at the 7 h mark; however, a minor rise in OD was noted in the treated groups, where bacteria treated at MOI of 0.001 and 100 showed an increase in OD towards the end of the experiment. According to Caflisch and Patel (2019), a phage is the only antibacterial agent that can proliferate over time using a bacterial host, and low MOI causes a slight increase in bacterial growth in contrast to higher MOI. This is attributed to the fact that a phage with a high MOI can identify and eradicate the bacteria more quickly than one with a low MOI. In this study, the MOIs 0.01, 0.1, 1 and 10 eventually destroyed the bacteria more successfully than MOIs 0.001 and 100.

According to Tian *et al.* (2021), biofilms are crucial to bacterial pathogenesis and contribute to infection persistence and increased antibiotic resistance. Bacteriophages have shown promise in eliminating *P. aeruginosa* biofilms (Singh *et al.*, 2025). According to the current results, RM_Ps3 exhibited strong antibiofilm activity against *P. aeruginosa*, demonstrating its possible use in the management of *Pseudomonas* infections. Bacteriophages may have antibiofilm function as they produce phage enzymes that break down extracellular matrix polymers like proteins and polysaccharides (Tian *et al.*, 2021). Bacteriophages have the ability to encode polysaccharide depolymerase, selectively breaking down macromolecular carbohydrates on the bacterial membrane (Islam *et al.*, 2024). Similar to this, bacteriophages generate endolysins that hydrolyze bacterial peptidoglycan, preventing the production of cell walls (Liu *et al.*, 2023). Bacteriophages may also generate enzymes that prevent *P. aeruginosa* from sensing quorum, preventing the creation of biofilms. It's interesting to note that lytic phages persist in their lytic activity against persister cells in biofilms, characterized by low metabolic activity (Chegini *et al.*, 2020). By the end, it appears that bacteriophages are a good choice for combating persistent biofilms. The RM_Ps3 phage's capacity to both stop the formation of biofilms and disintegrate those that have already been developed suggested that it may be used as a treatment to stop this kind of infection linked to biofilm formation. After an incubation period, bacterial biofilm development was remarkably lower at all assessed MOIs, compared to the untreated culture. These results are consistent with those of Mohamed *et al.* (2025), who found that phage vB_Ps_ZCPS13 appreciably reduced biofilm development for all tested MOI doses. The antibiofilm activity of phage RM_Ps3 is linked to a previous study, which revealed that phages can interfere with the initial stages of biofilm formation through interfering with bacterial adhesion or synthesis of enzymes that act on the extracellular matrix of a biofilm (Santiago and Donlan, 2020). This confirmed the successful application of RM_Ps3 phage in management of biofilm infections caused by *P. aeruginosa.*

Conclusions and Recommendations

This work revealed that phage RM_Ps3 can potentially be used as antibacterial and antibiofilm agent for treatment of MDR *P. aeruginosa*, particularly those infections linked to biofilms formation. The phage showed strong lytic efficacy versus 86% of the pathogenic strains examined and displayed considerable effectiveness in preventing and eliminating biofilms. *In vitro*, this study exhibited strong phage therapeutic activity throughout a broad spectrum of MOIs, showing the greatest efficiency at lower MOIs. Additionally, the phage displayed strong stability to a range of unfavorable environmental conditions, where it retained its efficacy despite exposure to varying pH and temperature levels. These results revealed that RM_Ps3 can be applied as an alternative for other medication in controlling carbapenem resistant *P. aeruginosa*. We recommend conductance of more research studies on phage genome sequencing and cocktailing of this phage with other phages to achieve its successful treatment approaches on a wide-range of MDR- *P. aeruginosa*.

Acknowledgments

We would like to sincerely acknowledge the Zewail City CMP team for their invaluable help during this research.

Novelty Statement

The novelty of this study lies in the inhibition of growth and biofilm formation of carbapenem resistant *P. aeruginosa* isolates collected from local hospital in Egypt using a highly lytic *Pseudomonas* phage isolated from sewage water.

Author's Contribution

RMS: Data curation, formal analysis, investigation, methodology, writing the original draft, review and editing. IMA: Methodology. ABB, AE, AA and MMG: Conceptualization and supervision. All authors read, revised, and approved the final manuscript.

Funding source
No external financial support was provided for this study.

Ethical approval
Ethical approval was obtained from the Research Ethics Committee of the Department of Microbiology, Faculty of Science, Ain Shams University under the code: ASU-SCI/MICR/2025/11/01.

Generative AI or AI-assisted technology statement
The authors declare that no generative AI was used in the creation of this manuscript.

Conflict of interests
The authors have declared no conflicts of interest.

References

Abdelaziz, S.M., Aboshanab, K.M., Yahia, I.S., Yassien, M.A. and Hassouna, N.A., 2021. Correlation between the antibiotic resistance genes and susceptibility to antibiotics among the carbapenem-resistant gram-negative pathogens. Antibiotics (Basel, Switzerland), 10(3): 255. https://doi.org/10.3390/antibiotics10030255

Abdelghafar, A., El-Ganiny, A., Shaker, G. and Askoura, M., 2023. Isolation of a bacteriophage targeting *Pseudomonas aeruginosa* and exhibits a promising *in vivo* efficacy. AMB Express, 13(1): 79. https://doi.org/10.1186/s13568-023-01582-3

Abdelrahman, F., Makky, S., Teba, H.E., Agwa, M.M., Abd-El-Aziz, M.M., Awad, R., Hassan, Y.Y., Abdelsattar, A.S., Connerton, I.F. and El-Shibiny, A., 2025. Potential of vB_Pa_ZCPS1 phage embedded in situ gelling formulations as an ocular delivery system to attenuate *Pseudomonas aeruginosa* keratitis in a rabbit model. J. Contr. Release Off. J. Contr. Release Soc., 380: 52–70. https://doi.org/10.1016/j.jconrel.2025.01.091

Abedon, S.T. and Thomas-Abedon, C., 2010. Phage therapy pharmacology. Curr. Pharma. Biotechnol., 11(1): 28–47. https://doi.org/10.2174/138920110790725410

Abedon, S.T., García, P., Mullany, P. and Aminov, R., 2017. Editorial: Phage therapy: Past, Present and future. Front. Microbiol., 8: 981. https://doi.org/10.3389/fmicb.2017.00981

Afify, F.A., Shata, A.H., Aboelnaga, N., Osama, D., Elsayed, S.W., Saif, N.A., Mouftah, S.F., Shawky, S.M., Mohamed, A.A., Loay, O. and Elhadidy, M., 2024. Emergence of carbapenem resistant gram-negative pathogens with high rate of colistin resistance in Egypt: A cross sectional study to assess resistance trends during the COVID-19 pandemic. J. Genet. Eng. Biotechnol., 22(1): 100351. https://doi.org/10.1016/j.jgeb.2024.100351

Aghaee, B.L., Mirzaei, M.K., Alikhani, M.Y. and Mojtahedi, A., 2021. Sewage and sewage-contaminated environments are the most prominent sources to isolate phages against *Pseudomonas aeruginosa*. BMC Microbiol., 21(1): 132. https://doi.org/10.1186/s12866-021-02197-z

Akremi, I., Merabishvili, M., Jlidi, M., Haj Brahim, A., Ben Ali, M., Karoui, A., Lavigne, R., Wagemans, J., Pirnay, J.P. and Ben Ali, M., 2022. Isolation and characterization of lytic *Pseudomonas aeruginosa* bacteriophages isolated from sewage samples from Tunisia. Viruses, 14(11): 2339. https://doi.org/10.3390/v14112339

Alemayehu, D., Casey, P.G., McAuliffe, O., Guinane, C.M., Martin, J.G., Shanahan, F., Coffey, A., Ross, R.P. and Hill, C., 2012. Bacteriophages φMR299-2 and φNH-4 can eliminate *Pseudomonas aeruginosa* in the murine lung and on cystic fibrosis lung airway cells. mBio, 3(2): e00029–e12. https://doi.org/10.1128/mBio.00029-12

Alharbi, N.M. and Ziadi, M.M., 2021. Wastewater as a fertility source for novel bacteriophages

against multi-drug resistant bacteria. Saudi J. Biol. Sci., 28(8): 4358–4364. https://doi.org/10.1016/j.sjbs.2021.04.025

Al-Orphaly, M., Hadi, H.A., Eltayeb, F.K., Al-Hail, H., Samuel, B.G., Sultan, A.A. and Skariah, S., 2021. Epidemiology of multidrug-resistant *Pseudomonas aeruginosa* in the Middle East and North Africa region. mSphere, 6(3): e00202-21. https://doi.org/10.1128/mSphere.00202-21

Alqahtani, A., 2023. Bacteriophage treatment as an alternative therapy for multidrug-resistant bacteria. Saudi Med. J., 44(12): 1222–1231. https://doi.org/10.15537/smj.2023.44.12.20230366

Arumugam, S.N., Manohar, P., Sukumaran, S., Sadagopan, S., Loh, B., Leptihn, S. and Nachimuthu, R., 2022. Antibacterial efficacy of lytic phages against multidrug-resistant Pseudomonas aeruginosa infections in bacteraemia mice models. BMC Microbiol., 22(1): 187. https://doi.org/10.1186/s12866-022-02603-0

Ata-Vural, I., Üsküdar, G.A., Yiğit, A.A., Kul, O. and Başustaoğlu, A., 2025. Evaluating the therapeutic potential of a novel bacteriophage cocktail against carbapenem-resistant *Pseudomonas aeruginosa* in a murine burn wound infection model. BMC Microbiol., 25(1): 682. https://doi.org/10.1186/s12866-025-04435-0

Barman, P., Chopra, S. and Thukral, T., 2018. Direct testing by VITEK® 2: A dependable method to reduce turnaround time in Gram-negative bloodstream infections. J. Lab. Phys., 10(3): 260–264. https://doi.org/10.4103/JLP.JLP_11_18

Basha, A., El-Sherbiny, G.M. and Mabrouk, M.I., 2020. Phenotypic characterization of the Egyptian isolates extensively drug-resistant *Pseudomonas aeruginosa* and detection of their metallo-β-lactamases encoding genes. Bull. Natl. Res. Cent., 44: 117. https://doi.org/10.1186/s42269-020-00350-8

Caflisch, K.M. and Patel, R., 2019. Implications of bacteriophage- and bacteriophage component-based therapies for the clinical microbiology laboratory. J. Clin. Microbiol., 57(8): e00229-19. https://doi.org/10.1128/JCM.00229-19

Chegini, Z., Khoshbayan, A., Taati-Moghadam, M., Farahani, I., Jazireian, P. and Shariati, A., 2020. Bacteriophage therapy against *Pseudomonas aeruginosa* biofilms: A review. Ann. Clin. Microbiol. Antimicrob., 19(1): 45. https://doi.org/10.1186/s12941-020-00389-5

Chen, L., Yuan, S., Liu, Q., Mai, G., Yang, J., Deng, D., Zhang, B., Liu, C. and Ma, Y., 2018. *In vitro* design and evaluation of phage cocktails against *Aeromonas salmonicida*. Front. Microbiol., 9: 1476. https://doi.org/10.3389/fmicb.2018.01476

Davis, R. and Brown, P.D., 2016. Multiple antibiotic resistance index, fitness and virulence potential in respiratory *Pseudomonas aeruginosa* from Jamaica. J. Med. Microbiol., 65(4): 261–271. https://doi.org/10.1099/jmm.0.000229

Dini, C., and de Urraza, P.J., 2013. Effect of buffer systems and disaccharides concentration on *Podoviridae coliphage* stability during freeze drying and storage. Cryobiology, 66(3): 339–342. https://doi.org/10.1016/j.cryobiol.2013.03.007

Echeverría-Vega, A., Morales-Vicencio, P., Saez-Saavedra, C., Gordillo-Fuenzalida, F. and Araya, R., 2019. A rapid and simple protocol for the isolation of bacteriophages from coastal organisms. MethodsX, 6: 2614–2619. https://doi.org/10.1016/j.mex.2019.11.003

El-Sherif, H.M., Elsayed, M., El-Ansary, M.R., Aboshanab, K.M., El-Borhamy, M.I. and Elsayed, K.M., 2022. BioFire FilmArray BCID2 versus VITEK-2 system in determining microbial etiology and antibiotic-resistant genes of pathogens recovered from central line-associated bloodstream infections. Biology, 11(11): 1573. https://doi.org/10.3390/biology11111573

Fayez, M.S., Hakim, T.A., Zaki, B.M., Makky, S., Abdelmoteleb, M., Essam, K., Safwat, A., Abdelsattar, A.S. and El-Shibiny, A., 2023. Morphological, biological, and genomic characterization of *Klebsiella pneumoniae* phage vB_Kpn_ZC2. Virol. J., 20(1): 86. https://doi.org/10.1186/s12985-023-02083-2

Fong, K., Wong, C.W.Y., Wang, S. and Delaquis, P., 2021. How broad is enough: The host range of bacteriophages and its impact on the agri-food sector. PHAGE (New Rochelle, N.Y.), 2(2): 83–91. https://doi.org/10.1089/phage.2020.0036

Glen, K.A. and Lamont, I.L., 2021. β-lactam resistance in *Pseudomonas aeruginosa*: Current status, future prospects. Pathogens (Basel, Switzerland), 10(12): 1638. https://doi.org/10.3390/pathogens10121638

Hemmati, J., Nazari, M., Abolhasani, F. S., Ahmadi, A. and Asghari, B., 2024. In vitro investigation of relationship between quorum-sensing system genes, biofilm forming ability, and drug resistance in clinical isolates of *Pseudomonas aeruginosa*. BMC Microbiol., 24(1): 99. https://doi.org/10.1186/s12866-024-03249-w

Huang, Y., Wang, W., Zhang, Z., Gu, Y., Huang, A., Wang, J. and Hao, H., 2022. Phage products for fighting antimicrobial resistance. Microorganisms, 10(7): 1324. https://doi.org/10.3390/microorganisms10071324

Islam, M.M., Mahbub, N.U., Shin, W.S. and Oh, M.H., 2024. Phage-encoded depolymerases as a strategy for combating multidrug-resistant *Acinetobacter baumannii*. Front. Cell. Infect. Microbiol., 14: 1462620. https://doi.org/10.3389/fcimb.2024.1462620

Ismael, N.M., Azzam, M., Abdelmoteleb, M. and El-Shibiny, A., 2024. Phage vB_Ec_ZCEC14 to treat antibiotic-resistant Escherichia coli isolated from urinary tract infections. Virol. J., 21(1): 44. https://doi.org/10.1186/s12985-024-02306-0

Jordá, J., Lorenzo-Rebenaque, L., Montoro-Dasi, L., Marco-Fuertes, A., Vega, S. and Marin, C., 2023. Phage-based biosanitation strategies for minimizing persistent salmonella and campylobacter bacteria in poultry. Animals, 13(24): 3826. https://doi.org/10.3390/ani13243826

Kadri, S.S., 2020. Key takeaways from the U.S. CDC's 2019 antibiotic resistance threats report for frontline providers. Crit. Care Med., 48(7): 939–945. https://doi.org/10.1097/CCM.0000000000004371

Kakasis, A. and Panitsa, G., 2019. Bacteriophage therapy as an alternative treatment for human infections. A comprehensive review. Int. J. Antimicrob. Agents, 53(1): 16–21. https://doi.org/10.1016/j.ijantimicag.2018.09.004

Kamer, A.M.A., Abdelaziz, A.A., Al-Monofy, K.B. and Al-Madboly, L.A., 2023. Antibacterial, antibiofilm, and anti-quorum sensing activities of pyocyanin against methicillin-resistant *Staphylococcus aureus*: *In vitro* and *in vivo* study. BMC Microbiol., 23(1): 116. https://doi.org/10.1186/s12866-023-02861-6

Khalifa, H.O., Soliman, A.M., Ahmed, A.M., Shimamoto, T., Nariya, H., Matsumoto, T. and Shimamoto, T., 2019. High prevalence of antimicrobial resistance in gram-negative bacteria isolated from clinical settings in Egypt: Recalling for judicious use of conventional antimicrobials in developing nations. Microb. Drug Resist. (Larchmont, N.Y.), 25(3): 371–385. https://doi.org/10.1089/mdr.2018.0380

Kirmusaoglu, S., 2016. Staphylococcal biofilms: Pathogenicity, mechanism and regulation of biofilm formation by quorum-sensing system and antibiotic resistance mechanisms of biofilm-embedded microorganisms. InTech. https://doi.org/10.5772/62943

Kropinski, A.M., Mazzocco, A., Waddell, T.E., Lingohr, E. and Johnson, R.P., 2009. Enumeration of bacteriophages by double agar overlay plaque assay. Methods Mol. Biol. (Clifton, N.J.), 501: 69–76. https://doi.org/10.1007/978-1-60327-164-6_7

Krumperman, P.H., 1983. Multiple antibiotic resistance indexing of *Escherichia coli* to identify high-risk sources of fecal contamination of foods. Appl. Environ. Microbiol., 46(1): 165–170. https://doi.org/10.1128/aem.46.1.165-170.1983

Kumar, S., Stecher, G. and Tamura, K., 2016. MEGA7: Molecular evolutionary genetics analysis version 7.0 for bigger datasets. Mol. Biol. Evolut., 33(7): 1870–1874. https://doi.org/10.1093/molbev/msw054

Kutter, E., 2009. Phage host range and efficiency of plating. Methods Mol. Biol. (Clifton, N.J.), 501: 141–149. https://doi.org/10.1007/978-1-60327-164-6_14

Ling, H., Lou, X., Luo, Q., He, Z., Sun, M. and Sun, J., 2022. Recent advances in bacteriophage-based therapeutics: Insight into the post-antibiotic era. Acta Pharma. Sinica B, 12(12): 4348–4364. https://doi.org/10.1016/j.apsb.2022.05.007

Litwin, A., Rojek, S., Gozdzik, W. and Duszynska, W., 2021. *Pseudomonas aeruginosa* device associated-healthcare associated infections and its multidrug resistance at intensive care unit of University Hospital: polish, 8.5-year, prospective, single-centre study. BMC Infect. Dis., 21(1): 180. https://doi.org/10.1186/s12879-021-05883-5

Liu, Y., Wang, J., Zhao, R., Liu, X., Dong, Y., Shi, W., Jiang, H. and Guan, X., 2024. Bacterial isolation and genome analysis of a novel Klebsiella quasipneumoniae phage in southwest China's karst area. Virol. J., 21(1): 56. https://

doi.org/10.1186/s12985-024-02321-1

Liu, H., Hu, Z., Li, M., Yang, Y., Lu, S. and Rao, X., 2023. Therapeutic potential of bacteriophage endolysins for infections caused by Gram-positive bacteria. J. Biomed. Sci., 30(1): 29. https://doi.org/10.1186/s12929-023-00919-1

Liu, S., Hon, K., Bouras, G.S., Psaltis, A.J., Shearwin, K., Wormald, P.J. and Vreugde, S., 2022. APTC-C-SA01: A novel bacteriophage cocktail targeting *Staphylococcus aureus* and MRSA biofilms. Int. J. Mol. Sci., 23(11): 6116. https://doi.org/10.3390/ijms23116116

Marashi, S.M.A., Nikkhahi, F., Hamedi, D. and Shahbazi, G., 2022. Isolation, characterization and *in vitro* evaluation of specific bacteriophages targeting extensive drug resistance strains of *Pseudomonas aeruginosa* isolated from septic burn wounds. Infect. Chemother., 54(1): 153–164. https://doi.org/10.3947/ic.2021.0132

Merabishvili, M., Vandenheuvel, D., Kropinski, A.M., Mast, J., De Vos, D., Verbeken, G., Noben, J.P., Lavigne, R., Vaneechoutte, M. and Pirnay, J.P., 2014. Characterization of newly isolated lytic bacteriophages active against *Acinetobacter baumannii*. PLoS One, 9(8): e104853. https://doi.org/10.1371/journal.pone.0104853

Merritt, J.H., Kadouri, D.E. and O'Toole, G.A., 2011. Growing and analyzing static biofilms. Curr. Protoc. Microbiol. 22: 1B.1.18. https://doi.org/10.1002/9780471729259.mc01b01s22

Mirzaei, M. and Nilsson, A.S., 2015. Isolation of phages for phage therapy: a comparison of spot tests and efficiency of plating analyses for determination of host range and efficacy. PloS one, 10(3): e0118557. https://doi.org/10.1371/journal.pone.0118557

Mohamed, A.A., El-Zayat, E.M. and El-Shibiny, A., 2025. Efficacy of phage vB_Ps_ZCPS13 in controlling Pan-drug-resistant Pseudomonas aeruginosa from urinary tract infections (UTIs) and eradicating biofilms from urinary catheters. Virol. J., 22(1): 236. https://doi.org/10.1186/s12985-025-02848-x

Pires, D.P., Melo, L., Vilas Boas, D., Sillankorva, S. and Azeredo, J., 2017. Phage therapy as an alternative or complementary strategy to prevent and control biofilm-related infections. Curr. Opin. Microbiol., 39: 48–56. https://doi.org/10.1016/j.mib.2017.09.004

Qin, S., Xiao, W., Zhou, C., Pu, Q., Deng, X., Lan, L., Liang, H., Song, X. and Wu, M., 2022. Pseudomonas aeruginosa: Pathogenesis, virulence factors, antibiotic resistance, interaction with host, technology advances and emerging therapeutics. Signal Transd. Target. Ther., 7(1): 199. https://doi.org/10.1038/s41392-022-01056-1

Ranjbar, R. and Alam, M., 2023. Antimicrobial resistance collaborators (2022). Global burden of bacterial antimicrobial resistance in 2019: A systematic analysis. Evidence-based nursing, ebnurs-2022-103540. Advance online publication. https://doi.org/10.1136/ebnurs-2022-103540

Rezk, N., Abdelsattar, A.S., Elzoghby, D., Agwa, M.M., Abdelmoteleb, M., Aly, R.G., Fayez, M.S., Essam, K., Zaki, B.M. and El-Shibiny, A., 2022. Bacteriophage as a potential therapy to control antibiotic-resistant *Pseudomonas aeruginosa* infection through topical application onto a full-thickness wound in a rat model. J. Genet. Eng. Biotechnol., 20(1): 133. https://doi.org/10.1186/s43141-022-00409-1

Rombouts, S., Volckaert, A., Venneman, S., Declercq, B., Vandenheuvel, D., Allonsius, C.N., Van Malderghem, C., Jang, H.B., Briers, Y., Noben, J.P., Klumpp, J., Van Vaerenbergh, J., Maes, M. and Lavigne, R., 2016. Characterization of novel bacteriophages for biocontrol of bacterial blight in leek caused by *Pseudomonas syringae* pv. porri. Front. Microbiol., 7: 279. https://doi.org/10.3389/fmicb.2016.00279

Santiago, A.J. and Donlan, R.M., 2020. Bacteriophage infections of biofilms of health care-associated pathogens: *Klebsiella pneumoniae*. EcoSal Plus, 9(1): 10.1128/ecosalplus.ESP-0029-2019. https://doi.org/10.1128/ecosalplus.esp-0029-2019

Schuetz, A.N., Ferrell, A., Hindler, J.A., Humphries, R. and Bobenchik, A.M., 2025. Overview of changes in the clinical and laboratory standards institute performance standards for antimicrobial susceptibility testing: M100 32nd and 33rd editions. J. Clin. Microbiol., 63(9): e0162323. https://doi.org/10.1128/jcm.01623-23

Shokri, D., Soleimani-Delfan, A. and Fatemi, S.M., 2017. Assessment of phage cocktails with extended host range activity against antibiotic resistant strains of *Pseudomonas aeruginosa*. Comp. Clin. Pathol., 26: 417–422. https://doi.org/10.1007/s00580-016-2394-y

Singh, B., Dahiya, M., Kumar, V., Ayyagari, A., Chaudhari, D.N. and Ahire, J.J., 2025. Biofilm and antimicrobial resistance: Mechanisms, implications, and emerging solutions. Microbiol. Res., 16(8): 183. https://doi.org/10.3390/microbiolres16080183

Soliman, R.M., Othman, B.A., Shoman, S.A., Azzam, M.I. and Gado, M.M., 2023. Biocontrol of multi-drug-resistant pathogenic bacteria in drainage water by locally isolated bacteriophage. BMC Microbiol., 23(1): 118. https://doi.org/10.1186/s12866-023-02847-4

Stepanović,S.,Vuković,D.,Hola,V.,DiBonaventura, G., Djukić, S., Cirković, I. and Ruzicka, F., 2007. Quantification of biofilm in microtiter plates: Overview of testing conditions and practical recommendations for assessment of biofilm production by *Staphylococci*. Acta Pathol. Microbiol. Immunol. Scand., 115(8): 891–899. https://doi.org/10.1111/j.1600-0463.2007.apm_630.x

Taati-Moghadam, M., Khoshbayan, A., Chegini, Z., Farahani, I. and Shariati, A., 2020. Bacteriophages, a new therapeutic solution for inhibiting multidrug-resistant bacteria causing wound infection: Lesson from animal models and clinical trials. Drug Design, Dev. Ther., 14: 1867–1883. https://doi.org/10.2147/DDDT.S251171

Tang, H.J., Chen, C.C., Ko, W.C., Yu, W.L., Chiang, S.R. and Chuang, Y.C., 2011. *In vitro* efficacy of antimicrobial agents against high-inoculum or biofilm-embedded meticillin-resistant *Staphylococcus aureus* with vancomycin minimal inhibitory concentrations equal to 2 μg/mL (VA2-MRSA). Int. J. Antimicrob. Agents, 38(1): 46–51. https://doi.org/10.1016/j.ijantimicag.2011.02.013

Tian, F., Li, J., Nazir, A. and Tong, Y., 2021. Bacteriophage: A promising alternative measure for bacterial biofilm control. Infect. Drug Resist., 14: 205–217. https://doi.org/10.2147/IDR.S290093

Tripathi, A.M., Tyagi, A., Kumar, A., Singh, A., Singh, S., Chaudhary, L.B. and Roy, S., 2013. The internal transcribed spacer (ITS) region and trnH-psbA [corrected] are suitable candidate loci for DNA barcoding of tropical tree species of India. PloS one, 8(2): e57934. https://doi.org/10.1371/journal.pone.0057934

Venkataraman, S., Shahgolzari, M., Yavari, A. and Hefferon, K., 2025. Bacteriophages as targeted therapeutic vehicles: Challenges and opportunities. Bioengineering, 12(5): 469. https://doi.org/10.3390/bioengineering12050469

Wannasrichan, W., Htoo, H.H., Suwansaeng, R., Pogliano, J., Nonejuie, P. and Chaikeeratisak, V., 2022. Phage-resistant *Pseudomonas aeruginosa* against a novel lytic phage JJ01 exhibits hypersensitivity to colistin and reduces biofilm production. Front. Microbiol., 13: 1004733. https://doi.org/10.3389/fmicb.2022.1004733

Wei, Y., Li, Z., Lao, J., Huang, J., Chen, H., Li, J., Deng, Y., Mao, X., Ma, R., Wu, Y., Tan, Y., Li, X., Lu, Y., Jiang, S. and Wang, X., 2025. Isolation and characterization of *Pseudomonas* phage HJ01 and its therapeutic efficacy in canine pyoderma. BMC Vet. Res., 21(1): 443. https://doi.org/10.1186/s12917-025-04877-8

Xu, Z., Ding, Z., Zhang, Y., Liu, X., Wang, Q., Shao, S. and Liu, Q., 2023. Shelf-life prediction and storage stability of Aeromonas bacteriophage vB_AsM_ZHF. Virus Res., 323: 198997. https://doi.org/10.1016/j.virusres.2022.198997

Zaki, B.M., Fahmy, N.A., Aziz, R.K., Samir, R. and El-Shibiny, A., 2023. Characterization and comprehensive genome analysis of novel bacteriophage, vB_Kpn_ZCKp20p, with lytic and anti-biofilm potential against clinical multidrug-resistant Klebsiella pneumoniae. Front. Cell. Infect. Microbiol., 13: 1077995. https://doi.org/10.3389/fcimb.2023.1077995

Zalewska-Piątek, B., 2023. Phage therapy challenges, opportunities and future prospects. Pharmaceuticals (Basel, Switzerland), 16(12): 1638. https://doi.org/10.3390/ph16121638

Zhang, Y., Wang, R., Hu, Q., Lv, N., Zhang, L., Yang, Z., Zhou, Y. and Wang, X., 2024. Characterization of *Pseudomonas aeruginosa* bacteriophages and control hemorrhagic pneumonia on a mice model. Front. Microbiol., 15: 1396774. https://doi.org/10.3389/fmicb.2024.1396774

Zhu, M., Hao, C., Zou, T., Jiang, S. and Wu, B., 2025. Phage therapy as an alternative strategy for oral bacterial infections: A systematic review. BMC Oral Health, 25(1): 44. https://doi.org/10.1186/s12903-024-05399-9